PRELIMINARY MODEL STUDIES OF THE MAGNETOSPHERE OF JUPITER: PIONEER 10

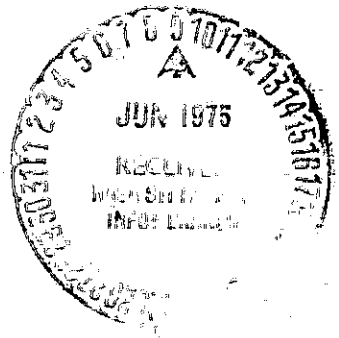

Douglas E. Jones

and

John G. Melville

Dept. of Physics and Astronomy

Brigham Young University

Provo, Utah

March, 1975

Introduction

The Pioneer 10 spacecraft passed within 2.84 Jovian radii (R_J) of the planet Jupiter on December 4, 1973. Extensive observations of the Jovian magnetic field and its interaction with the solar wind plasma were made while the spacecraft was within about 100 R_J of the planet. The magnetosphere was found to be severely stretched due to the presence of an intense current sheet, which was particularly evident during the outbound passage of Pioneer 10 near the dawn terminator (Smith, et al., 1974). Plots of the angle between the orientation of the outbound field and the radius vector from the planet to the spacecraft showed a strong tendence for the field to become radial at large distances from the planet (see Fig. 8, Smith,et al., 1974). A similar trend has also been seen in both the inbound and outbound Pioneer 11 data (Smith,et al.,1975; Jones,et al.,1975). We report here some preliminary work on a mathematical model of the magnetosphere of Jupiter which is based upon the Pioneer 10 outbound data. A preliminary model study related to the outbound Pioneer 10 data has also been reported by Goertz,et al.,(1974). However, we have noted some fundamental conceptual errors in their study and it is also the purpose of this paper to report a correction of this earlier analysis. We will also discuss some of the implications of the radial field configuration inferred from the Pioneer 10 and 11 data.

The Method

Since it is always true that

$$\nabla \cdot \vec{B} = 0$$

one can represent $\vec{B}$ by an expression of the form

$$\vec{B} = \nabla f \times \nabla g$$

where f and g are scalar functions of the coordinates that are sometimes referred to as Euler potentials (Euler, 1769; Truesdell, 1954; Stern, 1966). The utility of this manner of representing $\vec{B}$ lies in the fact that since $\vec{B}$ is tangent to the intersection of the surfaces f = constant and g = constant, this affords a direct

method of evaluating the shape of the lines of force. For example, for a dipole in spherical coordinates, we have

$$f_D = \frac{M \sin^2\theta}{\rho}$$

where $\rho = R/R_J$, and

$$g = \phi$$

(In cylindrical coordinates, ρ will represent the dimensionless component of $\vec{R}$ that is perpendicular to the axis of the dipole.) The f function can be easily manipulated into the well-known constant L representation of a dipole field line, namely

$$\rho = L \sin^2\theta$$

Although, the law of superposition holds for magnetic fields, this is not generally true for the functions f and g, i.e.,

$$\nabla F \times \nabla G = \nabla\left(\sum_i f_i\right) \times \nabla\left(\sum_i g_i\right) \neq \sum_i (\nabla f_i \times \nabla g_i)$$

Alternatively, one notes that

$$\nabla f \times \nabla g = \nabla \times (f \nabla g)$$

so that the vector potential $\vec{A}$ is related to the f and g functions through

$$\vec{A} = f \nabla g$$

For axi-symmetric fields, f is independent of ϕ and $g = \phi$. The vector potential in spherical coordinates is then

$$\vec{A}_{spher.} = \frac{f(\rho,\theta)}{\rho \sin\theta}\,\hat{\phi}$$

and in cylindrical coordinates,

$$\vec{A}_{cyl.} = \frac{f(\rho,z)}{\rho}\,\hat{\phi}$$

For axi-symmetric fields, or f functions sharing the same g function, one writes

$$\vec{A} = \sum_i f_i \nabla g$$

or, alternatively

$$\vec{B} = \nabla \times \left(\sum_i f_i \nabla g\right) = \nabla\left(\sum_i f_i\right) \times \nabla g$$

We write with B_D being the dipole field,

$$\vec{B} = \vec{B}_D + \vec{B}_1 + \vec{B}_2$$

or $$\vec{B} = \nabla(f_D + f_1) \times \nabla g_1 + \nabla f_2 \times \nabla g_2$$

so that the perturbation field $\vec{B}_p$ is given by

$$\vec{B}_p = \vec{B} - \vec{B}_D$$
$$= \vec{B}_1 + \vec{B}_2$$
$$= \nabla f_1 \times \nabla g_1 + \nabla f_2 \times \nabla g_2$$

$\vec{B}_1$ represents the axi-symmetric portion of the perturbation field and $\vec{B}_2$ the component contributing to the spiralling.

Spherical Polar Coordinate Model

In spherical coordinates, we have

$$\vec{B}_1 = \frac{1}{\rho^2 \sin\theta} \frac{\partial f_1}{\partial \theta} \hat{r} - \frac{1}{\rho \sin\theta} \frac{\partial f_1}{\partial \rho} \hat{\theta}$$

$$\vec{B}_2 = \frac{k}{\rho \sin\theta} \frac{\partial f_2}{\partial \theta} \hat{\phi}$$

Since there is clearly spiralling of the field (Smith et al., 1974), we have written

$$g_p = g_1 + g_2$$
$$= \phi + k\rho$$

where $k\rho$ represents the spiralling. Because B_1 and B_D share the same g function, and therefore superposition holds for the respective f functions, we will concentrate on these components of the field only. The function $F = f_1 + f_D$ will then represent meridional plane projections of the measured field.

In deriving an f_1 function, we start with a component of the perturbation field whose functional form may be easily deduced from the data. Since the radial component of the field decreased and at times reversed, which is consistent with passage into a thin current sheet (Smith, et al., 1974), a functional form for b_ρ that is consistent with these factors (see also Bird, 1975) is

$$b_\rho = \frac{A}{\rho^a} \tanh \frac{\cos\theta}{\cos\theta_0}$$
$$= \frac{1}{\rho^2 \sin\theta} \frac{\partial f_1}{\partial \theta}$$

Then

$$f_1 = -\frac{A \cos\theta_0}{\rho^{a-2}} \left[\log \cosh \frac{\cos\theta}{\cos\theta_0} + C(\rho) \right]$$

and $$b_\theta = -\frac{1}{\rho \sin\theta}\frac{\partial f_1}{\partial \rho}$$

$$= \frac{(a-2)A\cos\theta_0}{\rho^a \sin\theta}\left[\log\cosh\frac{\cos\theta}{\cos\theta_0} + C(\rho)\right] - \frac{A\cos\theta_0}{\rho^{a-1}\sin\theta}\frac{\partial C(\rho)}{\partial \rho}$$

At $\theta = \pi/2$,

$$b_\theta = \frac{(a-2)A\cos\theta_0}{\rho^a}C(\rho) - \frac{A\cos\theta_0}{\rho^{a-1}}\frac{\partial C}{\partial \rho}$$

For

$$C(\rho) = \frac{C}{\rho^b}$$

we have

$$b_\theta = \frac{AC\cos\theta_0}{\rho^{a+b}}(a-2+b)$$

The f function corresponding to the axi-symmetric portion of the perturbation field is then given by

$$f_1 = -\frac{A\cos\theta_0}{\rho^{a-2}}\left[\log\cosh\frac{\cos\theta}{\cos\theta_0} + \frac{C}{\rho^b}\right]$$

From the Pioneer 10 outbound data, we find that the constants for f_1 are approximately

a = 1.70

b = 1.10

A = 7700

C = 770

$\cos\theta_0$ = 0.025

Although fitting the Pioneer 10 outbound data quite well, this F function exhibited rather anomalous behavior at high latitudes. Since the expression for b_ρ can include additional functions of θ which are small near $\theta = \pi/2$ (i.e., functions of $\cos\theta$) one could write

$$b_\rho = \frac{A}{\rho^a}\tanh\frac{\cos\theta}{\cos\theta_0} + \cos\theta\, h(\rho,\theta)$$

Following this lead, alternate functions can be derived. One of several which fits the data reasonably well is

$$f_1 = -\frac{\lambda \cos\theta_0}{\rho^{a-2}}\left[\log\cosh\frac{\cos\theta}{\cos\theta_0} + \frac{Ce^{1-\sin\theta}}{\rho^{b}}\right]$$

where the constants are the same as those listed above. The corresponding F function is plotted in Figure 1 with $M = 4 \times 10^5$ (Smith, et al., 1974; 1975). Although this function exhibits better behavior near the magnetic axis, it is still unsatisfactory here. Replacing $Ce^{1-\sin\theta}/\rho^b$ by $-\log\cosh(1/\cos\theta_0)$ produces an f_1 which matches the $b\rho$ data and is well behaved at 0^0, but insufficient southward field results because effects due to magnetopause currents have not been included in the model. Clearly an additional f function is needed, but infinite series techniques will likely be required.

Neglecting the presence of the magnetopause, the last closed field line crosses the magnetic equator at $\rho_c = 440$ for the preceding models. Under these conditions magnetic field lines originating at higher latitudes would not cross the equator and would therefore be considered as being open.

The Cylindrical Coordinate Model

Goertz, et al. (1974) have developed a model in cylindrical coordinates. For this case, the axi-symmetric portion of the perturbation field is given by

$$\vec{B}_1 = -\frac{1}{\rho}\frac{\partial f_1}{\partial z}\hat{\rho} + \frac{1}{\rho}\frac{\partial f_1}{\partial \rho}\hat{k}$$

As before, a functional form for b_ρ that is consistent with the current sheet data, etc., is

$$b_\rho = \frac{A}{\rho^a}\tanh z/D$$

where the current sheet half-width, D, could be some function of ρ, i.e.

$$D = D_0 \rho/\rho_0$$

for a constant angular width sheet, or in general

$$D = D_0\left(\rho/\rho_0\right)^k$$

Since

$$b_\rho = -\frac{1}{\rho}\frac{\partial f_1}{\partial z}$$

then

$$f_1 = -\frac{AD}{\rho^{a-1}}\log\cosh z/D + C(\rho)$$

The corresponding function for b_z is then

$$b_z = \frac{AD(a-1)}{\rho^{a+1}}\log\cosh z/D - \frac{bAz}{\rho^{a+1}}\tanh z/D + \frac{\partial C(\rho)}{\rho\,\partial\rho}$$

Note that for $z/D \geq 3$, log cosh z/D is very nearly z/D - ln 2, so that

$$b_z\Big|_{z/D\geq 3} = \frac{AD}{\rho^{a+1}}(a-b-1)\frac{z}{D} - \frac{AD(a-1)}{\rho^{a+2}}\ln 2 + \frac{\partial C(\rho)}{\rho\,\partial\rho}$$

Plotting b_ρ versus ρ for all $z/D \geq 3$, and b_z versus ρ for fixed values of z/D, allows one to determine the constants in f_1. Goertz, et al. (1974) have plotted b_z in this manner and find

$$a+b+1 = 2.77$$

$$C(\rho) = -\frac{15\,AD}{\rho^{a-1}}$$

so that

$$f_1 = -\frac{AD}{\rho^{a-1}}\left(\log \cosh 3/\delta + 15\right)$$

However, Goertz et al. (1974) have plotted b_s versus ρ, where

$$b_s = b_\rho \sqrt{1 + b_\phi^2/b_\rho^2}$$

and

$$b_\phi = -k\rho\, b_\rho$$

As a result, they obtain a power law representation of the component parallel to the magnetic equator which lies in the curved surface represented by

$$\phi + k\rho = \text{constant}$$

However, the resulting f will be for such surfaces, does not represent an axi-symmetric field, and therefore cannot appropriately be added to the dipole f function, which is axi-symmetric. That is, the f functions to be added must share the same g function. Goertz, et al. (1974) found that

$$\frac{b_\phi}{\rho \cdot b_\rho} = -8 \times 10^{-3}$$

and hence

$$b_s = b_\rho \sqrt{1 + (8 \times 10^{-3}\rho)^2}$$

Since they found

$$b_s \propto \rho^{-1.67}$$

over the range $\rho = 20$ to $\rho = 80$, the corresponding ρ dependence for b_ρ should be corrected by the factor $\rho^{0.11}$, or

$$b_\rho \propto \rho^{-1.78}$$

so that

a = 1.78

b = -0.01

As a check on this, we determined the power law dependence of b_0 on ρ directly and obtained values for a, A, and b of 1.75, 1.0 X 10^4, and +0.02 respectively for the range ρ = 30 to 80. Combining our results with those of Goertz, et al. (1974) we find that f_1 is given by

$$f_1 = -\frac{1.0 \times 10^4}{\rho^{0.75}} \left(\log \cosh \frac{3}{D} + 15\right) \qquad (30 \leq \rho \leq 80)$$

where b has been assumed equal to zero, and, based upon one well defined current dip, D_0 has been set equal to 1 in units of Jovian radii. The total F function representing the axi-symmetric portion of the field is then

$$F = \frac{M\rho^2}{(\rho^2+z^2)^{3/2}} - \frac{1.0 \times 10^4}{\rho^{0.75}} \left(\log \cosh \frac{3}{D} + 15\right)$$

A plot of F is shown in Fig. 2. Applying the same conditions as for the spherical model, the above model predicts that the last closed field line will cross the magnetic equator at $\rho_c \cong 160$. Using a = 1 2/3 and A = 7.5 X 10^3, Goertz, et al. (1974) obtain $\rho_c \cong 150$.

The Currents

The current configuration in the magnetosphere can be obtained simply from Ampere's law. Using the field expressions derived from the several f_1 functions one can obtain the configuration of the intense current sheet that exists at the magnetic equator as well as the volume currents. The ϕ components of the internal magnetospheric current system is found in each case to consist of a sheet current term plus a volume current term, where the sheet term for the spherical model is

$$J_\phi\Big|_{sheet} = \frac{A \sin\theta}{\mu_0 R_J \rho^{A+1} \cos\theta_0} \operatorname{sech}^2 \frac{\cos\theta}{\cos\theta_0}$$

and for the cylindrical model

$$J_\phi\Big|_{sheet} = \frac{A}{\mu_0 R_J D \rho^a} \operatorname{sech}^2 z/D$$

Although the volume terms are negligible near the magnetic equator, they dominate near the magnetic polar axis. This is clearly an artifact of each model which will disappear when proper account of the magnetopause currents and the inner cutoff radius of the current sheet or disc are included.

Mathematically terminating the field at the magnetopause allows one to solve for the magnetopause currents, and the corresponding boundary field direction

can be determined for the several models and compared with the data. For example, a function, $t(\rho/\rho_o)$, which can terminate the field arbitrarily abruptly is

$$t(\rho/\rho_o) = \frac{1 + \tanh d\,(1 - \rho/\rho_o)}{2}$$

so that the terminated field, $\vec{B}'$, is given by

$$\vec{B}' = t(\rho/\rho_o)\,\vec{B}$$

Here ρ_o is the radial distance to the magnetopause (as a first approximation we assume the magnetopause boundary to be spherical) and d relates to the thickness of the boundary. In principle, $\vec{B}$ should be the total field. However, we still neglect the ϕ component of the perturbation field.

The above function terminates the preceding azimuthal currents at $\rho = \rho_o$ and in addition provides the magnetopause currents,- i.e., for the spherical model

$$J_\phi\Big|_{m.p.} = \frac{-d}{2\mu_o R_J \rho_o}\left[\operatorname{sech}^2 d\,(1 - \rho/\rho_o)\right] B_\theta$$

and for the cylindrical model (here $\rho = \sqrt{x^2 + y^2}$, normalized)

$$J_\phi\Big|_{m.p.} = \frac{-d}{2\mu_o R_J \rho_o}\left[\operatorname{sech}^2 d\left(1 - \frac{\sqrt{\rho^2+z^2}}{\rho_o}\right)\right]\left[\frac{z B_\rho - \rho B_z}{\sqrt{\rho^2+z^2}}\right]$$

we find that B_θ for the spherical model is positive at all values of θ so that the corresponding magnetopause current is clockwise, as viewed from the magnetic pole, at all latitudes. Hence, just prior to the magnetopause boundary the predicted field direction is southward,- as is observed by both Pioneers 10 and 11 (Smith, et al.,1974;1975). On the other hand, the bracketed term contained in

the magnetopause expression for the cylindrical model becomes negative at magnetic latitudes greater than about 20^{o} so that the direction of the magnetopause current flow reverses from a clockwise direction at lower latitudes to a counter clockwise direction at higher latitudes. The corresponding field just inside the boundary is predicted to point northward at latitudes greater than 20^{o} and southward at lower latitudes. Such a prediction appears to be in disagreement with the data although it is interesting to note that prior to the outbound magnetopause crossings by Pioneer 11 there were intervals approaching 8 hours during which the magnetospheric fields pointed north of radial by roughly 20^{o}. However, these are likely transient features related to a (possibly) northward component of the solar wind flow velocity.

Discussion

Since the functions plotted in Figs. 1 and 2 were derived from the Pioneer 10 outbound data, they were developed from data taken within about 20^0 of the magnetic equator and over the radial range $20 \leq \rho \leq 80$, and qualitatively represent the magnetospheric field configuration in meridional planes that lie near the dawn terminator. However, one notes that the models also qualitatively fit the Pioneer 11 data quites well which extends the latitude range of the functions to perhaps 40^0 (the Pioneer 11 inbound data is qualitatively very similar to the Pioneer 10 outbound data) and to about 40^0 [illegible] of the dawn meridian. As is evident from the figures, both models should be considered unreliable at latitudes greater than about 45^0.

A basic difference between the two models is the fact that one is for a constant angular width current sheet (the spherical coordinate model, Fig. 1) while the other is for a constant thickness current sheet (the cylindrical coordinate model, Fig. 2). Likely the actual case lies somewhere between these two current sheet configurations. Both permit the current sheet to exist to the center of the planet although it must be cut off at some inner radius $\rho \geq 2$, since one would not expect the sheet to exist within the centrifugal-gravitational balance distance of several radii.

Another basic difference involves the direction of flow of the magnetopause currents and the corresponding direction of the magnetopause field. Predictions based upon the spherical model are more consistent with the measurements.

There are also a number of factors regarding the constants derived for the models that should be mentioned. For example, in the case of the cylindrical coordinate model, the value of c in f_1 is determined from b_z versus ρ at constant z/D, but this requires a knowledge of D. The evaluation of the constants a, A,

and b depends c tically upon the accurate determination of the actual power law dependence of D on ρ. The current sheet half-width is one of the most uncertain parameters and its dependence upon ρ is particularly difficult to determine directly from the plots of $\vec{B}$ versus ρ. The constants contained in the expression for f_1 are self-consistent and the model appears to establish the ρ independence of D. Similar comments can be made regarding the constant angular width model as well. Unfortunately, a brief study of the variation of the widths of the field dips has not shed much light on this crucial point except that the data tend to favor the cor-tant angular width model.

In the study by Goertz et al. (1974), the determination of a and D (their b_0) from a plot of b_s instead of b_ρ causes the resulting function that is to represent the shape of the field in meridional planes to be a mixture of f functions requiring different g functions. On the other hand, in our determination of these constants for the cylindrical model, we have used only f functions that have the same g function. Because the spiralling of the field was not excessive, the disagreement with the results of Goertz et al. (1974) is not great, and a comparison of the plots of the field lines shows them to be quite similar.

Any interpretation regarding the value of ρ_c (where $B_\perp = 0$) that is derived from the models should be viewed with caution since the model fits the data only out to about 80 or 85 R_J, and hence these cutoff radii should be considered as possible artifacts of the models. An artifact of this kind is meaningless because the magnetopause currents have been neglected in the derivation of the f functions. As noted earlier, it is tempting to assume that field lines leaving the planet at higher magnetic latitudes than those related to ρ_c are open field lines and that they merge with the interplanetary field. But the data show that the field lines are southward at the magnetopause, suggesting that they are closed

by the magnetopause currents. In the sense of field lines and particle trapping, these lines clearly will not have trapped particles on them. The last closed field line which could contain trapped particles should be the one which crosses the equator just prior to the magnetopause boundary.

The particles in the intense equatorial current sheet likely result from plasma flow due to the combined action of a Jovian "polar wind," much like that postulated for Earth (Banks and Holzer, 1969), plus the strong centrifugal force caused by the large size and rapid rotation of the magnetosphere. The balance of pressures at the magnetopause likely must include that exerted by a radial flow of polar wind ions moving parallel to the essentially radial field lines in the magnetosphere. Perhaps such a plasma flow also provides a significant stabilizing influence for the large scale magnetosphere configuration reported here, since one would otherwise expect the solar wind to blow the high latitude field lines back into the tail because of the relatively weak magnetic pressure exerted at the magnetopause (Smith, et al., 1974). A study of the Pioneer 11 outbound data will provide some important information in this regard, although much higher latitude data are clearly needed.

Further studies of the magnetosphere will likely require the use of perturbation techniques (Stern, 1967) in order to obtain more well behaved functions at high latitudes and to allow for a non-spherical magnetopause boundary. Other studies being conducted at the present time will merge models developed for the range $1 \leq \rho \leq 6$ with the magnetospheric models reported here. In this regard, magnetospheric studies establish reasonable estimates of the magnetospheric current systems and detailed attempts at merging the two programs will establish, among other things, the inner cutoff radius of the current sheet.

This research was supported in part by the National Aeronautics and Space Administration under NASA-Ames contract NAS2-7358.

LIST OF REFERENCES

Banks, P.M. and T.E. Holzer. High latitude plasma transport: the polar wind. J. Geophys. Res. 74, 6317, 1969.

Bird, M.K. Solar wind access to the plasma sheet along the flank of the magnetotail. Planet. Space Science 23, 27, 1975.

Euler, L. Sectio secunda de principiis motus fluidorum, Novi Comentarii Acad. Sci Petrolotance, 14, 270, 1769; reprinted in Leonhardi Euleri Opera Omnia, Series II, vol. 13, p. 73, Swiss Society for Natural Sciences, 1955.

Goertz, C.K., B.A. Randall, M.F. Thomsen. A model for the Jovian magnetic field. Paper presented at the Fall, 1974, Meeting of the American Geophysical Union, Dec 12-17, 1974.

Jones, D.E., E.J. Smith, L. Davis, Jr., P.J. Coleman, Jr., D.S. Colburn, P. Dyal and C.P. Sonett. Pioneer 11 measurements of Jupiters magnetic field. Paper presented at the Spring, 1975 meeting of the Utah Academy of Sciences, Arts and Letters, March 28, 1975 (abstract this issue of the proceedings).

Mihalov, J.D., H.R. Collard, D.D. McKibbin, J.H. Wolfe, and D.S. Intriligator. Preliminary Pioneer 11 encounter results from the Ames Research Center plasma analyzer experiment. To be published in Science, 1975.

O'Brien, V. Axi-symmetric magnetic fields and related problems. J. Franklin Institute 275, 24, 1963.

Smith, E.J., L. Davis, Jr., D.E. Jones, P.J. Coleman, Jr., D.S. Colburn, P. Dyal, C.P. Sonett, and A.M.A. Frandsen. The Planetary magnetic field and magnetosphere of Jupiter: Pioneer 10. J. Geophys. Res. 79, 3501, 1974.

Smith, E.J., L. Davis, Jr., D.E. Jones, P.J. Coleman, Jr., D.S. Colburn, P. Dyal, C.P. Sonett, Jupiters magnetic field, magnetosphere and interaction with the solar wind. To be published in Science, 1975.

Stern, D.P. The motion of magnetic field lines. Space Science Rev. 6, 147, 1966.

Stern, D. Geomagnetic Euler Potentials. J. Geophys. Res. 72, 3995, 1967.

Truesdell, C. The kinematics of vorticity, Indiana University Press, 1954.

Figure Captions

1. Meridional plane representation of the magnetospheric field as developed in a spherical coordinate representation. The solid and dashed arrows represent the average field direction measured at several points along the outbound trajectories of Pioneer 10 and 11, respectively. The shaded half-angular width portion near the magnetic equator represents a portion of the equatorial current sheet configuration assumed in this model, and a first order approximation to the magnetopause boundary is also indicated. Regions over which the function is reliable are indicated in the text. The curves leave the $\rho = 2$ sphere at equally spaced angular intervals.
2. Meridional plane representation of the magnetospheric field as developed in a cylindrical coordinate representation. The solid and dashed arrows represent the average field direction measured at several points along the outbound trajectories of Pioneer 10 and 11 respectively. The shaded half-width portion near the magnetic equator represents a portion of the equatorial current sheet configuration assumed in this model, and a first order approximation to the magnetopause boundary is also indicated. Regions over which the function is reliable are indicated in the text. The curves leave the = 2 sphere at equally spaced angular intervals.

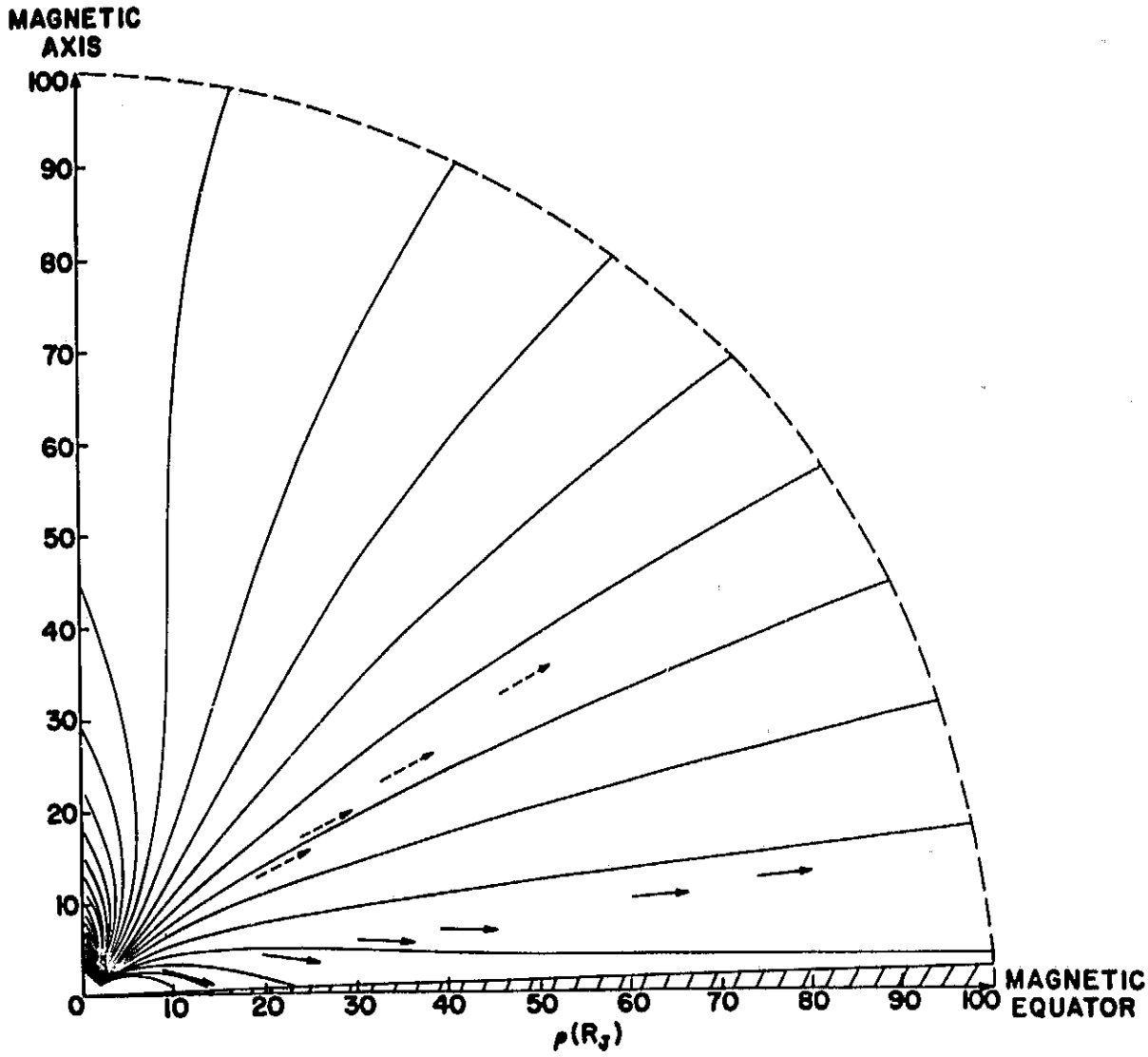
MAGNETIC
AXIS
100
90
80
70
60
50
40
30
20
10
0
10
20
30
40
50
60
70
80
90
100
MAGNETIC
EQUATOR
ρ(R_J)

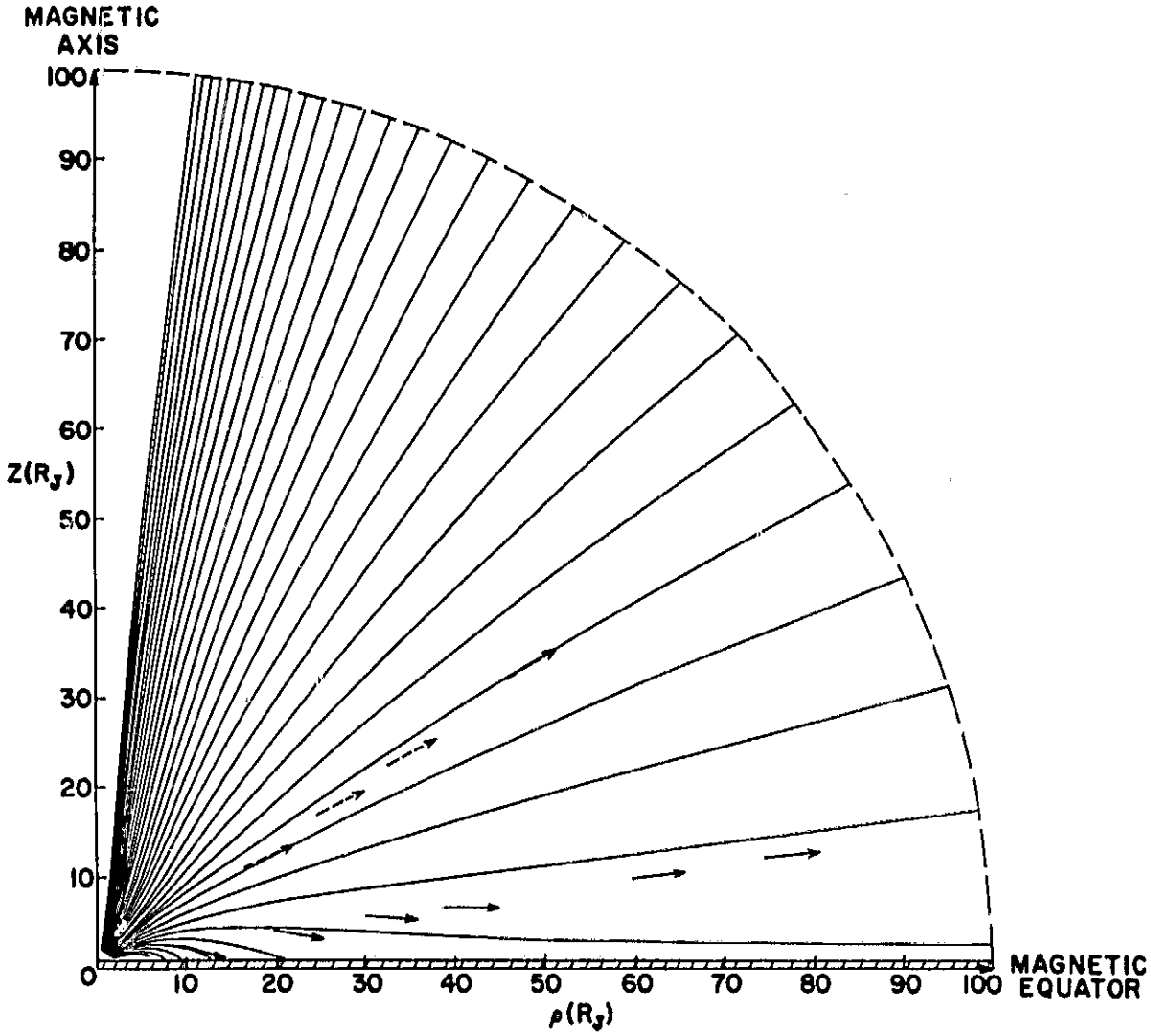
MAGNETIC
AXIS
100
90
80
70
60
Z(R_J)
50
40
30
20
10
0
10
20
30
40
50
60
70
80
90
100
MAGNETIC
EQUATOR
ρ(R_J)